

Frequency Dependence of AC Transport Properties of Films of Cobalt Iron Prussian Blue Analogues

Joel C. A. Reid,* Pedro A. Quintero, and Mark W. Meisel

Department of Physics and NHMFL, University of Florida, Gainesville, FL, 32611-8440

(Dated: August 1, 2014)

Prussian blue analogues (PBAs) have the interesting property of temperature dependent and photo-induced spin phase transitions. A measurement of the AC transport properties at fixed frequency and as a function of temperature of PBAs reveals a possible new method of measuring these phase transitions and spin states. The DC measurement of the conductivity shows a similar temperature dependence to the AC capacitance indicating a possible phase switch. This work aims to qualify the frequency dependence of the AC transport properties of a NaCoFe PBA.

1. INTRODUCTION

Sodium cobalt iron Prussian blue analogue (NaCoFe PBA) are molecules that have the general formula $\text{Na}_j\text{Co}_k[\text{Fe}_m(\text{CN})_6]_l \cdot n\text{H}_2\text{O}$, and an example is given in Fig. 1. Interestingly, NaCoFe PBA can be optically and thermally induced to change its spin phase. The resulting spin phase transition occurs due to an electron charge transfer from the iron atom to the cobalt atom, thereby changing the low spin state to the high spin state as shown in Fig. 2. Specifically, this process can be either thermally induced or realized by a radiation with light at low temperature, and it is known as a charge transfer induced spin transition (CTIST). At low temperature, initially both atoms are in a low spin state ($S_{\text{Fe/Co}} = 0$), and after the charge transfer induced by irradiation, the PBA is said to be in a high spin state because iron will have a spin state of $\frac{1}{2}$ ($S_{\text{Fe}} = \frac{1}{2}$), while the cobalt will have a $\frac{3}{2}$ spin state ($S_{\text{Co}} = \frac{3}{2}$).

Most importantly, the CTIST effect, Fig. 2, results in a change in the molecular properties such as bond length. This structural modification creates a measurable change in the transport properties such as conductivity (σ) and capacitance (C). Thus, spin phase transition can be observed by measuring the transport properties, whose frequency dependences will be explored in this work.

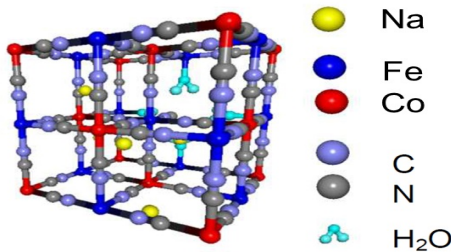


FIG. 1: NaCoFe PBA Structure (molecular formula: $\text{Na}_2\text{Co}_4[\text{Fe}(\text{CN})_6]_{3.3} \cdot 14\text{H}_2\text{O}$).

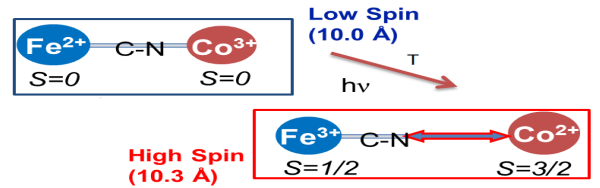


FIG. 2: Light/temperature induced CTIST electron transfer diagram and phase transition.

1.1. Temperature induced CTIST

At DC, the magnetic properties and the natural log of the resistivity (inverse conductivity) are expected to be approximately linear under small ranges of temperature. Data reported by O. Sato (Fig. 3) shows DC measurements of the resistivity and magnetic measurements for two different NaCoFe PBAs as they pass through their respective CTIST regions. The data deviates from the expected linear curve as the molecules change their geometry and bond lengths. The PBA, at either end of the CTIST, clearly has different transport properties because the slopes of the linear fits are different.

The NaCoFe PBA being explored in this work was synthesized by O. Risset [2] and has a slightly different chemical structure than the ones reported by O. Sato in Fig. 3. It behooves us then, to make a DC measurement of this new PBA sample to see if the CTIST region exists and where it occurs. Shown in Fig. 4 is data showing the DC measurements of the conductivity as the PBA passes through its CTIST region. For relatively small ranges of temperature the log of the conductivity as a function of temperature can once again, be approximated to a linear function. The CTIST region, where the data deviates from this expected trend, can be seen at around 230 – 260 K. Comparison between the data set in Fig. 4, and an AC measurement of the transport properties allows one to determine if the CTIST is visible using the AC voltage source.

*Electronic address: joelreid@ufl.edu

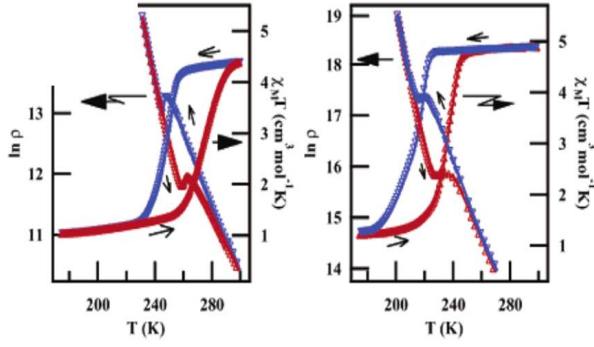


FIG. 3: Resistivity and magnetic measurements through the CTIST transition of NaCoFe PBAs, $\text{Na}_{0.5}\text{Co}_{1.25}[\text{Fe}(\text{CN})_6] \cdot 4.8\text{H}_2\text{O}$ (left panel) and $\text{Na}_{0.38}\text{Co}_{1.31}[\text{Fe}(\text{CN})_6] \cdot 5.4\text{H}_2\text{O}$ (right panel) as reported by O. Sato et al. [1] Reprinted with permission from O. Sato et al., J. Am. Chem. Soc. (2004) **126**, 13176. Copyright 2004 American Chemical Society.

At 1 kHz, AC measurement of the conductance, shown in shown in Fig. 5, shows a deviation in the same area as the DC measurement but the shape of the deviation is strange. As the PBA transitions from low spin to high spin phase, the DC measurement shows a sharp change through the CTIST (Fig. 4), whereas the AC measurement shows an almost sinusoidal change. To make matters worse, the AC capacitance shows a similar sharp change through the CTIST that the DC conductivity shows. It is possible then, that the conductance and capacitance undergoes a phase switch between DC and 1 kHz. Unravelling this puzzling phenomenon necessitates undergoing an AC frequency exploration.

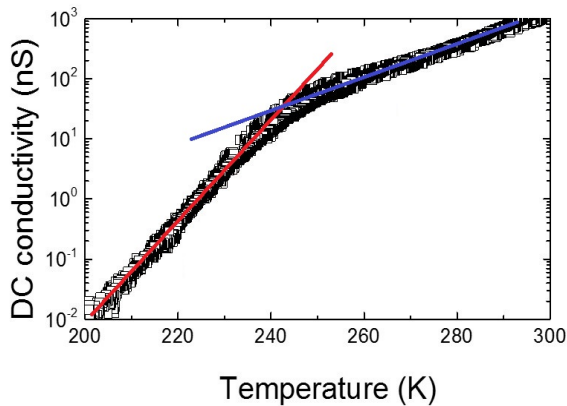


FIG. 4: DC conductivity measurement of NaCoFe PBA ($\text{Na}_2\text{Co}_4[\text{Fe}(\text{CN})_{3.3}] \cdot 14\text{H}_2\text{O}$).

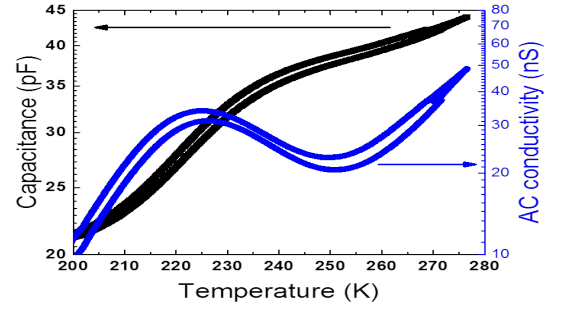


FIG. 5: AC measurement of NaCoFe PBA passing through a CTIST region at 1 kHz ($\text{Na}_2\text{Co}_4[\text{Fe}(\text{CN})_{3.3}] \cdot 14\text{H}_2\text{O}$).

1.2. Photo-induced CTIST

At temperatures below the phase transition temperature, the high spin state of the PBA is achievable by irradiating the sample with white light. During the irradiation, the PBA enters an excited state and gains a higher conductivity value (σ_I). After the light has been turned off, the PBA relaxes into and remains in the high spin state. This change is visible by measuring the conductivity. Prior to irradiation the conductivity value (σ_{PreI}) is different than the resulting conductivity value post irradiation (σ_{PostI}). Fig. 6 shows how this light induced CTIST effectively freezes the PBA in a high spin state until a critical temperature (T_c) of about 150 K is achieved. Afterwards, there is no linger effect, even after the temperature induced CTIST.

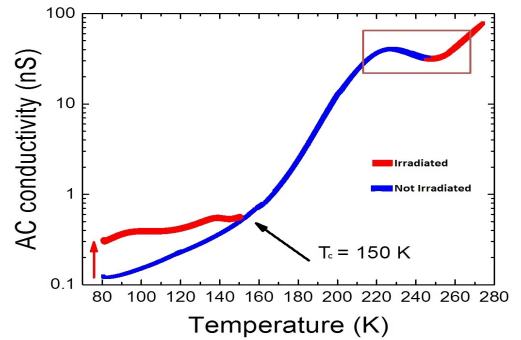


FIG. 6: Sample is first cooled to around 80 K and then irradiated for 15 minutes. The light is then turned off and data is collected after an hour has passed. Irradiation effect persists until around the temperature reaches around 150 K. Afterwards no discernible effects are measured.

Intriguingly, the magnitude of this irradiation CTIST effect has an initial temperature dependence. Data shown in Fig. 7 demonstrates that the strength of the irradiation effect decreases as one increases the initial irradiation temperature. One of the goals of this work is to characterize the frequency dependent effects on T_c and

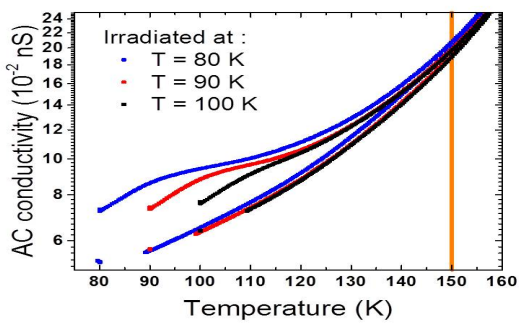


FIG. 7: Irradiation of NaCoFe PBA at initial temperatures of 80, 90 and 100 K.

in turn on the the effect on the persistence of the light effect. Evidently, to maximize the frequency dependent effects, it would be beneficial to evaluate at the lowest temperature possible.

2. EXPERIMENTAL DETAILS

2.1. Experimental Setup and Materials

The sample, after synthesis by O. Risset [2], is then drop casted onto a Indium tin oxide (ITO) transparent conducting substrate (see Fig. 8). Using silver epoxy, copper leads are connected to each end of the conducting substrate. The plate, along with a temperature probe and a resistive heater, is then lowered into the inner chamber of the Cryofab Dewar (Fig. 9). The Dewar contains three chambers which, in order from outer to inner, are the jacket, outer and inner chambers. The inner chamber contains the sample while the outer chamber contains helium gas and the jacket contains liquid nitrogen. The liquid nitrogen is used in conjunction with the resistive heater to control the temperature of the PBA. Helium is used in order to have a separation between the liquid nitrogen and the sample. The leads from the substrate are connected to a variable frequency capacitance bridge (See Fig. 10) while the temperature probe and the resistive heater leads are connected to the temperature controller. Both the capacitance bridge and the temperature controller are then connected to a computer where data is stored and collected.[3]

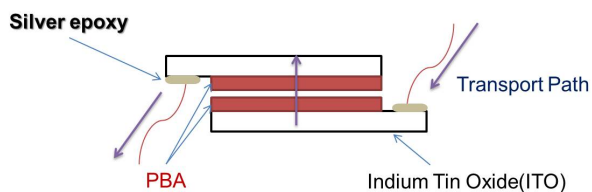


FIG. 8: A diagram showing the PBA on a conducting substrate.

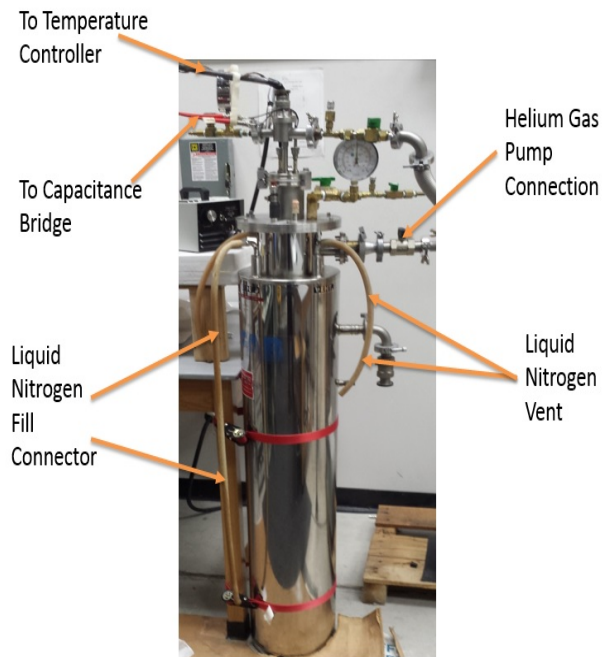


FIG. 9: Image showing the Cryofab Dewar that contains the PBA sample.

2.2. Procedure

First the PBA sample, the conducting disk, the resistive heater and the temperature probe is placed in the Cryofab Dewar inner chamber. Next the outer chamber is filled with Helium gas and finally the jacket is filled with liquid nitrogen. All data parameters (temperature, capacitance and conductance) are taken as functions of time. The temperature of the PBA is adjusted by adding liquid nitrogen to the outer jacket of Dewar. This setup causes the helium gas to cool and in turn causes the sample to cool. The sample is then heated and cool by adjusting the power output from the temperature controller

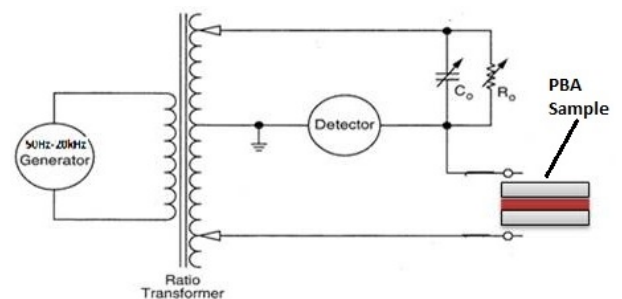


FIG. 10: Circuit diagram of a capacitance bridge. The capacitance bridge works by varying the standard resistor and capacitor until the detector measures a null. At this point the standard capacitor and resistor are equal in magnitude to the sample's capacitance and resistance.

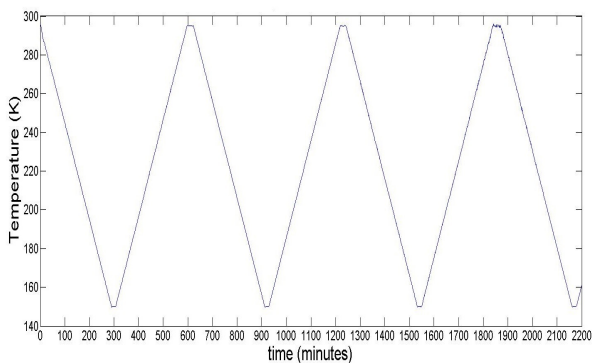


FIG. 11: A plot of temperature vs. time at 0.5K/min. During this temperature cycle, the frequency will cycle many times between specific frequencies between 50 Hz and 20 kHz. In the end time will be removed as the intermediate variable and data will be plotted as a function of temperature.

to the resistive heater. While taking data, the temperature controller is programmed to cycle between certain set points. At each set point the controller will wait until the temperature becomes steady [4]. An example of the temperature cycle is shown in Fig. 11. During this temperature cycle, the capacitance bridge will sweep through frequencies from 50 Hz to 20 kHz with near equal spacing on a logarithmic scale. All values are then recorded at once and given a time stamp. The data is saved to a file where it can be analyzed later. Using time as the intermediate variable, the capacitance and conductance can then be taken as functions of temperature.

3. RESULTS AND DISCUSSION

3.1. Variable Frequency Temperature induced CTIST

The capacitance plot (Fig. 14 in the appendix A) shows the capacitance as a function of temperature and frequency. The capacitance does not return to the same value as one sweeps the temperature. A possible reason for this effect is that the capacitance resulting from the leads attached to the PBA have non-trivial conductance. At this time, a definitive solution is not yet available and therefore the conductance will become the main focus of this work.

Fig. 15, shown in the appendix A, shows the frequency dependent plot of the conductance vs temperature. The phase transition measured previously (Fig. 5) was around 220 to 260K whereas here, the 1 kHz phase transition, seen in purple, is around 240 to 280 K. Another notable effect is the shift in the temperature dependent CTIST region as one increases the frequency.

We can conclude from these data sets that there is not a capacitance to conductance frequency dependent phase shift. We can also conclude that the reason for

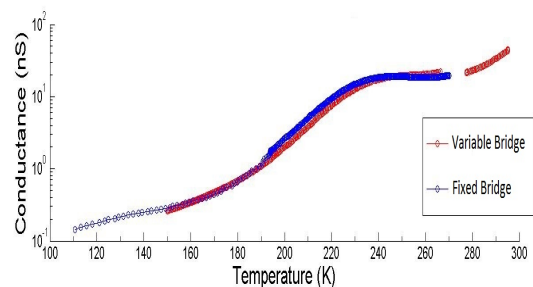


FIG. 12: A 1 kHz comparison of AC transport measurement of the 1 kHz AC Capacitance Bridge and the 50 Hz-20kHz AC Capacitance Bridge.

the shift in the 1 kHz data is not an effect from the equipment. The bridge used to take data in Fig. 5 was reused to take new data to compare. The result, shown in Fig. 12, is that the data are similar to within uncertainty. Differences arise from the sweep rate that each data set was taken at. Finally, it is not yet known how or why the frequency causes the unexpected shift in the temperature dependent CTIST region.

3.2. Variable Frequency Phot-induced CTIST

At 80 K, when irradiated with white light, the conductance follows the same trend at all frequencies as reported before in Fig. 6. Fig. 16 in appendix A shows that at all frequencies, the value the conductance falls to after the light has been turned off, is different than the value recorded before the sample was irradiated. While this effect holds true for all frequencies, both the magnitude of the difference between the pre-irradiated and post-irradiated conductance, given by

$$\Delta(f, T) = \sigma_{PostI}(f, T) - \sigma_{PreI}(f, T) \quad , \quad (1)$$

and the relative gain, given by

$$G(f, T) = \left(\frac{\Delta(f, T)}{\sigma_{PreI}(f, T)} \right) * 100\% \quad , \quad (2)$$

change with frequency. More interestingly, while the difference magnitude increases with frequency, the relative gain decreases with frequency. This effect could be due to some property of the material or possibly just a mathematical consequence caused by the difference in orders of magnitude of the pre-irradiation conductance at different frequencies. More analysis, such as a wider frequency range, could shed some light.

The persistent irradiation effect that was observed in Fig. 6, is also observed at all measured frequency. Fig. 17 shows the irradiation effect at different frequencies and while there are small differences in the critical temperature, all seem to occur before 180K. It is possible that they are all the same to within some uncertainty, however more analysis would need to be done to be sure.

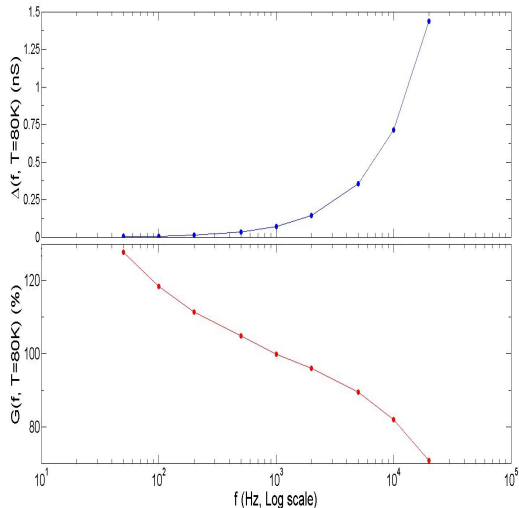


FIG. 13: Plots showing $\Delta(f, T = 80 \text{ K})$ and $G(f, T = 80 \text{ K})$ as functions of frequency.

4. CONCLUSION

There seems to be a strong frequency dependence on the location of the temperature CTIST and the magnitude of the difference between pre-irradiated conductance and post-irradiated conductance. It is still unclear how these effects may be quantified but qualitatively there is a strong need for recognition of the frequency dependence effect.

Acknowledgments

JCAR thanks the University of Florida REU program and all its associates for this summer research opportunity. JCAR also thanks Mackenzie W. Turvey, Marcus K. Peprah and Tatiana V. Brinzari for teaching invaluable techniques that are sure to be useful in the future. This work was supported, in part, by NSF DMR-1202033 (MWM), DMR-1157490 (NHMFL), and DMR-1156737 (UF REU Program).

-
- [1] O. Sato et al., *J. Am. Chem. Soc.* (2004) **126**, 13176.
 [2] Olivia N. Risset, Talham group, Department of Chemistry, University of Florida, Gainesville, FL, 32611-8440
 [3] The PBA and substrate are held in a Cryofab dewar and are connected BNC cables to a Andeen Hagerling capacitance bridge (AH 2700A, 50Hz to 20 kHz). The resistive heater and temperature probe are connected to a Lakeshore 325 Temperature Controller. Both the temperature controller and the capacitance bridge are connected to and controlled by a Windows XP Home Edition Dell desktop computer. Data analysis is done in Matlab 2013 edition.

- [4] Once the standard deviation of the last eight measurements of temperature falls below 1 K, the temperature is thought to be steady.

Appendix A: Large Plots

Expanded versions of Figs. 14-17 are given on the pages 6-7. The rest of this page is left intentionally blank.

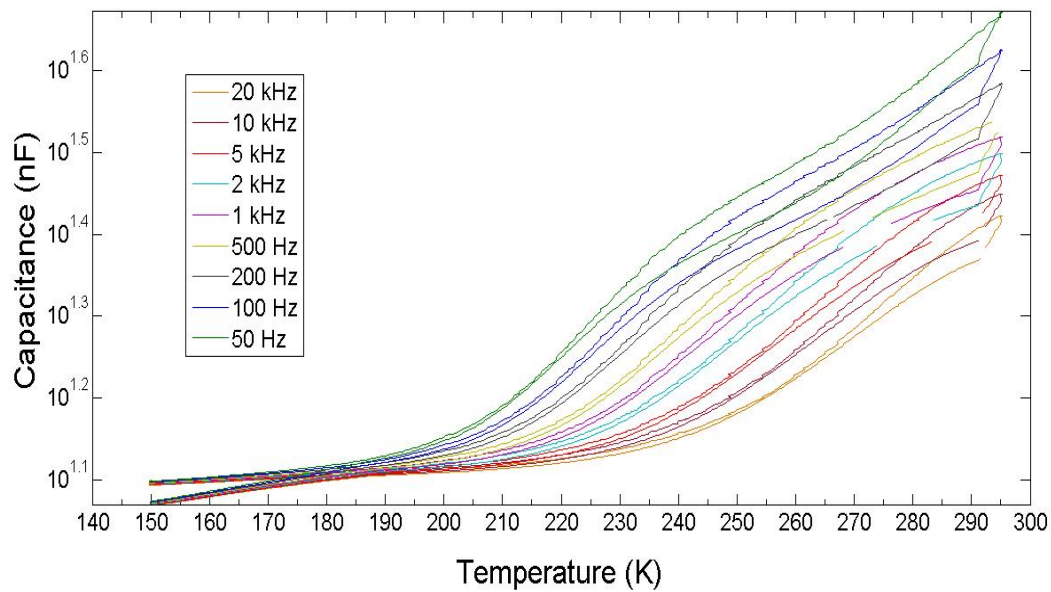


FIG. 14: A 625 minute plot at 0.5K/min of capacitance as a function of temperature and at varying frequencies.

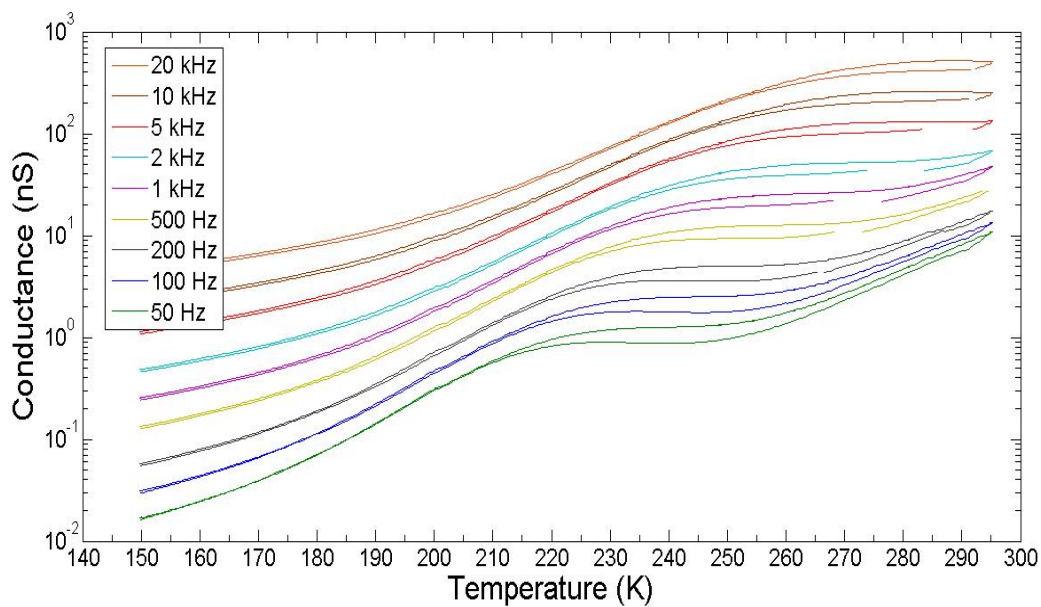


FIG. 15: A 625 minute plot at 0.5K/min of conductance as a function of temperature at varying frequencies.

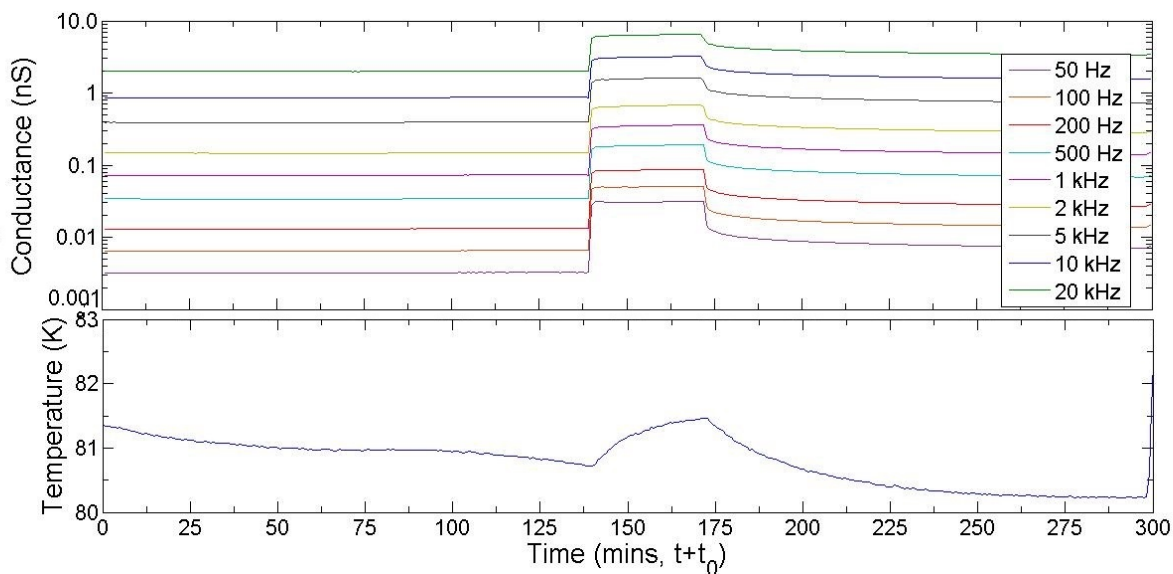


FIG. 16: Top shows the conductance as a function of time while the bottom shows the temperature as a function of time. $t_0 = 400$ mins. Light is turned on at approximately $t = 140$ mins and for a duration of 30 mins.

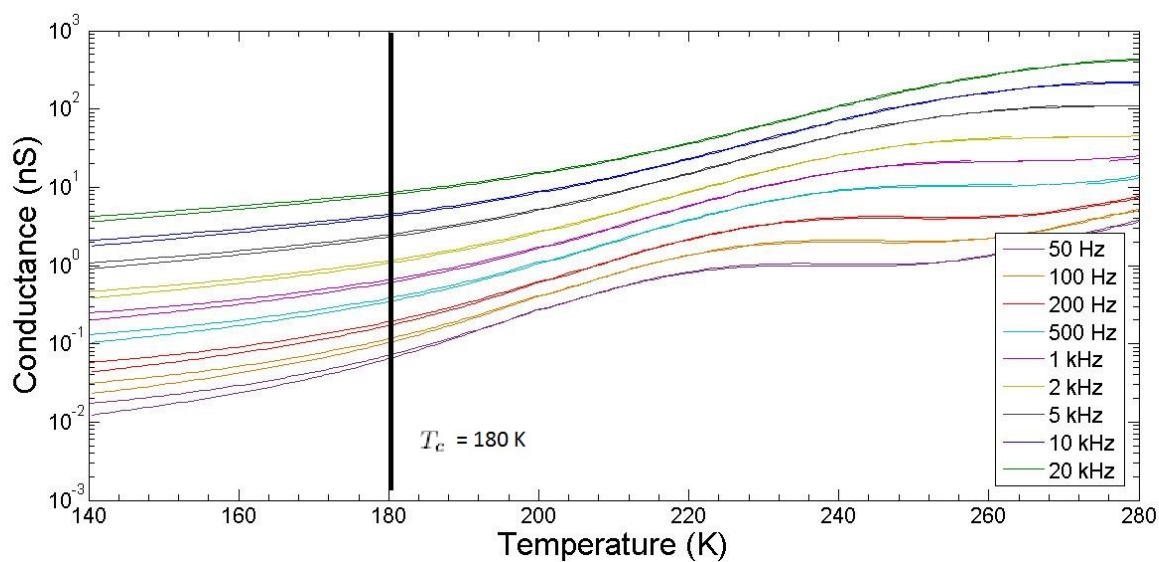


FIG. 17: Post irradiation Conductance sweep as a function of temperature. Sample was irradiated at 80K for 30 minutes. The light was then turned of and after a period of 125 minutes the temperature was increased then decreased back at a rate of 0.5K/min.